Biogeosciences

Open Access

EGU

Supplement of

An estuarine-tuned quasi-analytical algorithm (QAA-V): assessment and application to satellite estimates of SPM in Galveston Bay following Hurricane Harvey

Ishan D. Joshi and Eurico J. D'Sa

Correspondence to: Eurico J. D'Sa (ejdsa@lsu.edu)

Chlorophyll-a profiles along with depth-dependent mass-specific IOPs are necessary to create Rrs using Hydrolight® four component case-2 models (S1) (Mobley and Sundman 2013; Sathyendranath et al., 1989; Kirk 1994; Bukata et. al., 1995),

$$a_t(\lambda) = a_w(\lambda) + a_\phi(\lambda) + a_{NAP}(\lambda) + a_g(\lambda)$$
$$b_{bt}(\lambda) = b_{bw}(\lambda) + b_{b\phi}(\lambda) + b_{bNAP}(\lambda) \tag{S1}$$

Synthetic chlorophyll concentrations [Chl] (N=730) were obtained with 73 values and ranged between 1 to 40 mg m^{-3} with 10 repetitions to simulate random variability as observed in natural waters. A total of 730 phytoplankton absorption spectra (a_ϕ) were generated using six groups containing 83 in situ normalized a_ϕ spectra; random normalized spectrum selection among groups were based on modeled $a_\phi 440$, and the following bio-optical models (Bricaud et al., 1995; Fischer and Fell 1999; Mobley 1994) (Fig. S1; Table S1),

$$a_\phi^{Normalized}(\lambda) = \frac{a_\phi(\lambda)}{a_\phi 440}$$
$$a_\phi 440 = 0.06 \times [Chl]^{0.65} \times \Re(1,2)$$
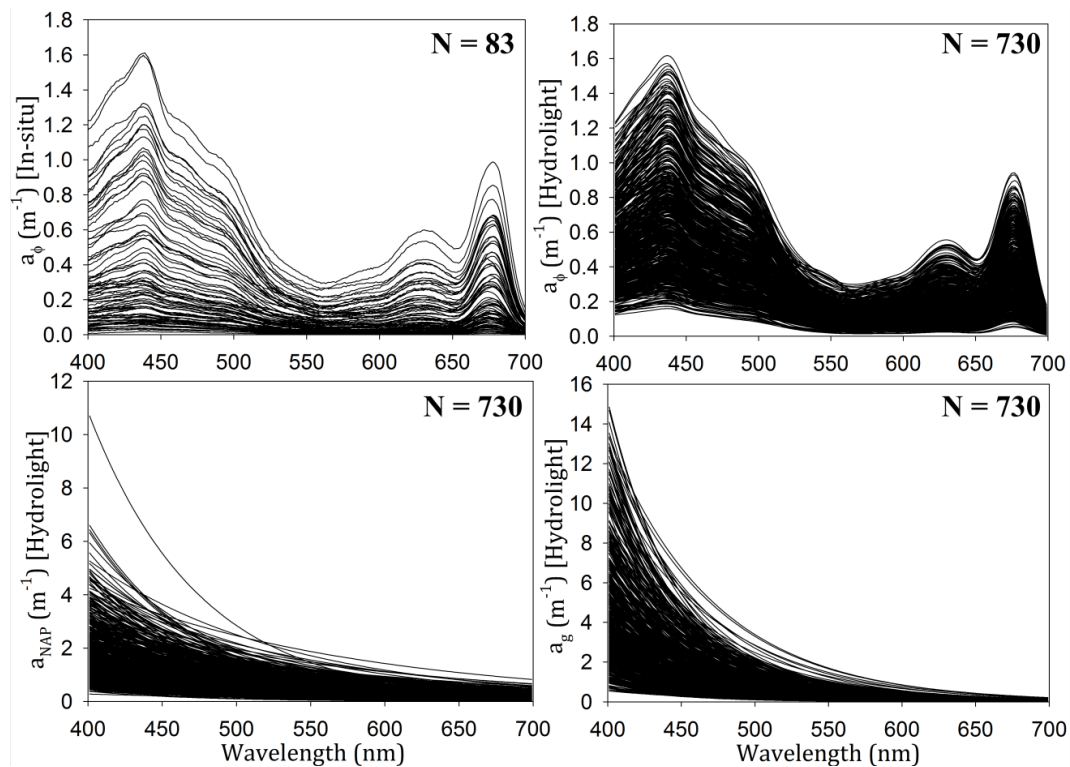$$a_\phi^*(\lambda) = \frac{a_\phi(\lambda)}{[Chl]} \tag{S2}$$

Figure S1. (a, b) *In situ* phytoplankton absorption spectra (N=83) were collected from CDOM-dominated Apalachicola Bay (USA) and sediment-dominated Barataria Bay (USA) to generate 730 simulated spectra for Hydrolight® four-component Case-2 model using Eq. 2, (c) modeled non-algal particle absorption spectra (N = 730) using Eq. 3, and (d) modeled CDOM absorption spectra (N = 730) using (S4).

Table S1: The conditions for allocating in-situ normalized-phytoplankton spectra ($a_\phi^{normalized}$) into 6 groups. $a_\phi 440$ is phytoplankton absorption at 440 nm.

Groups (Total spectra = 83)	Condition
1 (n=18)	$a_\phi 440 < 0.1$
2 (n=15)	$a_\phi 440 \geq 0.1$ & $a_\phi 440 < 0.2$
3 (n=12)	$a_\phi 440 \geq 0.2$ & $a_\phi 440 < 0.3$
4 (n=11)	$a_\phi 440 \geq 0.3$ & $a_\phi 440 < 0.5$
5 (n=16)	$a_\phi 440 \geq 0.5$ & $a_\phi 440 < 1.0$
6 (n=11)	$a_\phi 440 \geq 1.0$

Mass-specific non-algal particle absorption coefficients ($a_{NAP}^*(\lambda)$) were obtained with an exponential model (Roesler et al. 1989; Bricaud et al. 1995), where slope (S_{NAP}) used a random value between 0.005 - 0.015 as observed in natural waters ranging from oceanic to estuarine environments (Kirk 1994). The required $a_{NAP}440$ was modeled using $a_\phi 440$ based on a constant p_1 (= $a_{NAP}440/ a_\phi 440$) which was set to lie between 1 and 3.5 as generally observed in the two bays, e.g., $p_1 = 1$ represents pigment/CDOM-rich waters and $p_1 = 3.5$ represents sediment/CDOM-rich waters (S3).

$$a_{NAP}(\lambda) = a_{NAP}440 \times e^{-S_{NAP} \times (\lambda - 440)}$$
$$p1 = 1 + \frac{2.5 \times a_\phi 440 \times \Re(0,1)}{0.05 + a_\phi 440}$$
$$a_{NAP}^*(\lambda) = \frac{a_\phi(\lambda)}{[NAP]}$$
$$[NAP] = p1 \times [Chl] \qquad (S3)$$

CDOM absorption coefficient was modeled with an exponential model (Bricaud et al. 1981), where spectral slope (S_g) was chosen randomly between 0.01 to 0.025 as generally observed in various oceanic to productive estuarine environments (Kirk 1994; Babin et al., 2003) (Fig. S1d). $a_g 440$ was estimated from $a_\phi 440$ and a constant $p2$ (= $a_g 440 /a_\phi 440$). p_2 was set between 1 to 4.5 based on field data, e.g., p_2= 1 represents phytoplankton/sediment dominated waters and p_2 = 4.5 represents CDOM-rich waters (S4).

$$a_g(\lambda) = a_g 440 \times e^{-S_g \times (\lambda - 440)}$$
$$a_g 440 = p2 \times a_\phi 440$$
$$p2 = 1 + \frac{3.5 \times a_\phi 440 \times \Re(0,1)}{0.02 + a_\phi 440}$$
$$a_g^*(\lambda) = \frac{a_g(\lambda)}{[Chl]} \qquad (S4)$$

Mass-specific phytoplankton backscattering ($b_{b\phi}^*$) and non-algal particle back-scattering (b_{bNAP}^*) coefficients were obtained based on the oceanic models (IOCCG 2006; please see references therein) with no change, as insufficient observations were available for estuarine environments. Subsequently, these coefficients were then converted to respective back-scattering coefficients by multiplying phase function dependent values "0.005" and "0.0183" (S5 and S6) (Mobley 1994; Mobley and Sundman 2013),

$$b_{bNAP}^*(\lambda) = \frac{b_{NAP}(\lambda) \times 0.0183}{[NAP]} \qquad (S5)$$
$$b_{b\phi}^*(\lambda) = \frac{b_\phi(\lambda) \times 0.005}{[Chl]} \qquad (S6)$$

Hydrolight® simulations were then run with a case-2 model to generate Rrs using mass-specific IOPs, chlorophyll concentrations, dark bottom sediments, finite depth of 5 meters, sun zenith angle of 30°, no Raman scattering, and no chlorophyll fluorescence. A total of 169 erroneous spectra were suspected

possibly due to atypical combinations of CDOM, non-algal particles, and bottom reflectance; these were not used in further analysis.

References

IOCCG (2006). Remote Sensing of Inherent Optical Properties: Fundamentals, Tests of Algorithms, and Applications. Lee, Z. P. (ed.), Reports of the International Ocean-Colour Coordinating Group, No. 5, IOCCG, Dartmouth, Canada.

IOCCG report 5. http://www.ioccg.org/groups/lee_data.pdf

Section S2

Table S2: Comparison statistics between the QAA-V and QAA-v6 algorithms based on simulated Hydrolight® dataset (HL) and in-situ estuarine and near-shore dataset (IES). N= number of observations, RMSE=Root mean square error, MRE= mean relative error.

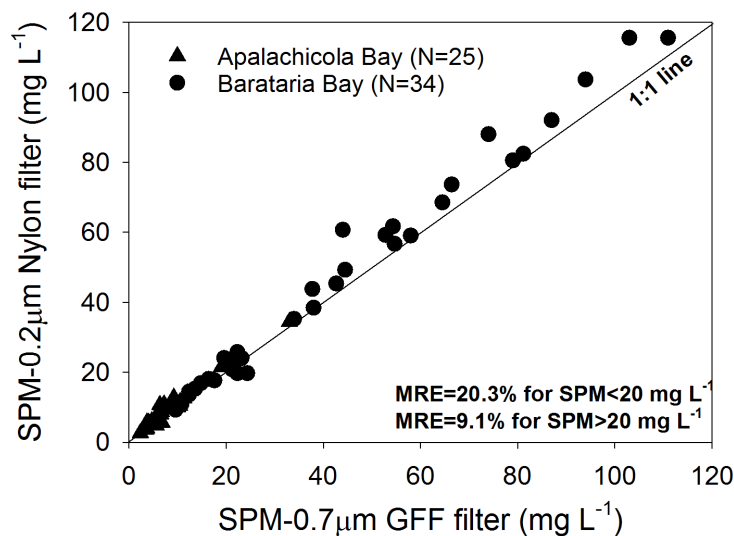|	N	$Bias_{log10}$ (m^{-1})		$RMSE_{log10}$ (m^{-1})		MRE (%)		R^2	
		QAA-V	QAA-v6	QAA-V	QAA-v6	QAA-V	QAA-v6	QAA-V	QAA-v6
Synthetic data									
$a_{tnw}411$	561	-0.028	-0.088	0.074	0.117	12.7	19.7	0.92	0.92
$a_{tnw}443$	561	-0.006	-0.071	0.071	0.106	12.7	17.7	0.91	0.90
$a_{tnw}489$	561	-0.003	-0.076	0.072	0.110	13.0	18.0	0.91	0.89
$a_{tnw}555$	561	-0.020	-0.118	0.096	0.149	16.3	23.9	0.87	0.87
$b_{btnw}411$	561	-0.041	-0.159	0.097	0.173	15.5	28.9	0.95	0.95
$b_{btnw}443$	561	-0.025	-0.130	0.086	0.152	14.4	25.3	0.95	0.94
$b_{btnw}489$	561	-0.017	-0.119	0.082	0.146	14.1	23.9	0.95	0.94
$b_{btnw}555$	561	-0.018	-0.121	0.089	0.153	14.9	23.9	0.94	0.93
IES dataset (Testing set: N = 219)									
$a_{tnw}443$	209	-0.023	-0.091	0.142	0.180	22.7	25.8	0.83	0.76
$a_{tnw}555$	209	-0.029	-0.124	0.190	0.249	34.3	47.5	0.72	0.63
$b_{btnw}532$	89	0.038	-0.049	0.173	0.174	26.0	34.6	0.70	0.67

Section S3

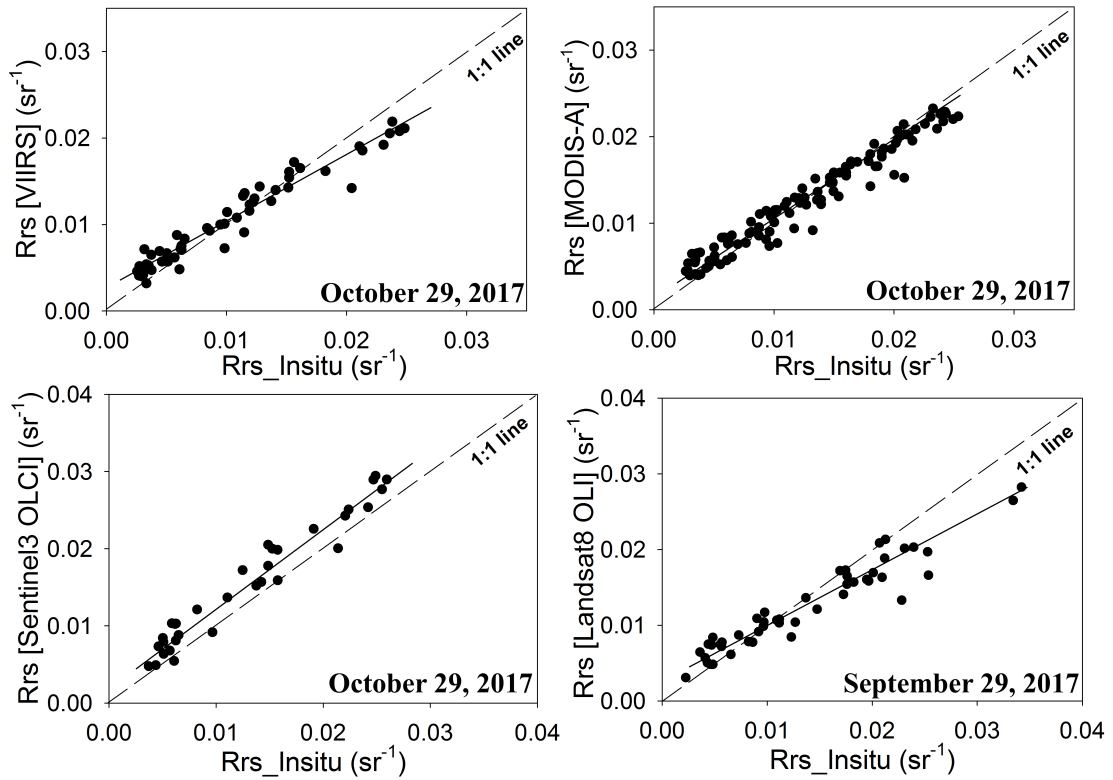Figure S2: A comparison of SPM concentration obtained with 0.2 μm Nylon filter and 0.7 μm GFF filters.

Section S4

Figure S3: Validation of the atmospheric corrected images that were used for generating maps of $a_{tnw}443$ and $bb_{tnw}470$ in Fig. 10 of the manuscript.